Infrared Studies of the Reaction of Methanesulfonic Acid with Trimethylamine on Surfaces

ARTICLE *in* ENVIRONMENTAL SCIENCE & TECHNOLOGY · DECEMBER 2013

Impact Factor: 5.33 · DOI: 10.1021/es403845b · Source: PubMed

4 AUTHORS, INCLUDING:

Kristine D Arquero
University of California, Irvine
5 PUBLICATIONS **32** CITATIONS
SEE PROFILE

Matthew L Dawson
University of California, Irvine
11 PUBLICATIONS **55** CITATIONS
SEE PROFILE

Barbara J Finlayson-Pitts
University of California, Irvine
233 PUBLICATIONS **7,288** CITATIONS
SEE PROFILE

Environmental Science & Technology

Article

pubs.acs.org/est

Infrared Studies of the Reaction of Methanesulfonic Acid with Trimethylamine on Surfaces

Noriko Nishino, Kristine D. Arquero, Matthew L. Dawson, and Barbara J. Finlayson-Pitts*

Department of Chemistry, University of California, Irvine, California, 92697-2025, United States

ABSTRACT: Organosulfur compounds generated from a variety of biological as well as anthropogenic sources are oxidized in air to form sulfuric acid and methanesulfonic acid (MSA). Both of these acids formed initially in the gas phase react with ammonia and amines in air to form and grow new particles, which is important for visibility, human health and climate. A competing sink is deposition on surfaces in the boundary layer. However, relatively little is known about reactions after they deposit on surfaces. We report here diffuse reflectance infrared Fourier transform spectrometry (DRIFTS) studies of the reaction of MSA with trimethylamine (TMA) on a silicon powder at atmospheric pressure in synthetic air and at room temperature, either in the absence or in the presence of water vapor. In both cases, DRIFTS spectra of the product surface species are essentially the same as the transmission spectrum obtained for trimethylaminium methanesulfonate, indicating the formation of the salt on the surface with a lower limit to the reaction probability of $\gamma > 10^{-6}$. To the best of our knowledge, this is the first infrared study to demonstrate this chemistry from the heterogeneous reaction of MSA with an amine on a surface. This heterogeneous chemistry appears to be sufficiently fast that it could impact measurements of gas-phase amines through reactions with surface-adsorbed acids on sampling lines and inlets. It could also represent an additional sink for amines in the boundary layer, especially at night when the gas-phase reactions of amines with OH radical and ozone are minimized.

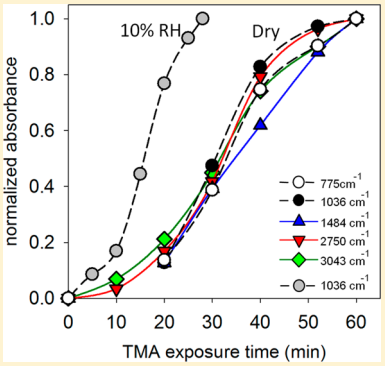

INTRODUCTION

Gaseous organic sulfur compounds such as dimethyl sulfide, dimethyl disulfide, dimethyl trisulfide, and methanethiol are generated by biological activity.[1−3] Although not as well documented, organosulfur compounds have also been measured from a variety of nonoceanic sources, including biomass burning; agricultural, industrial, and domestic activities; and diesel exhaust.[4−11] They are oxidized in air, mainly by OH radicals during the day and nitrate radicals at night, to form a variety of sulfur oxides, including sulfuric acid and methanesulfonic acid (MSA, $CH_3S(O)_2OH$).[12] Both of these acids have been measured in the gas phase, with sulfuric acid at concentrations[11,13−18] that are typically 10^5−10^7 molecules cm^{-3}, and MSA concentrations[11,13,14,16−18] that are about 10−100% of those of sulfuric acid.

There is increasing evidence that reactions of ammonia (NH_3) and amines with sulfuric acid in air significantly enhance the formation and growth of new particles compared to systems containing only sulfuric acid and water.[19−27,39] A similar observation has been reported for MSA reacting with amines.[28] This is important because particles have significant impacts on visibility[12,29] and human health,[30−32] as well as on climate.[33]

Amines have many biogenic and anthropogenic sources including marine organisms, biomass burning, animal husbandry, food industry, sewage, and vehicle exhaust, with the total estimated global emission of methyl, dimethyl, and trimethylamines (MA, DMA and TMA, respectively) being ∼300 Gg N a^{-1}.[34,35] While global emissions of these alkylamines are minor compared to NH_3 (5×10^4 Gg N a^{-1}), laboratory[22,25,36−39] and computational[39−41] studies suggest that these amines have a greater impact on new particle formation and growth than NH_3. These amines have been widely observed in ambient particles over a broad size range from a few nanometers[21] to approximately micrometer size particles in urban, suburban, rural, and coastal regions as well as over the ocean.[35]

Sinks for MSA/sulfuric acid and amines in air include not only their gas-phase reaction to form new particles, and uptake onto/into existing particles, but also deposition of the gases at the Earth's surface. In the boundary layer, there are many surfaces available in the form of built structures such as buildings and roads, as well as natural vegetation that can serve as substrates for deposition.[42−44] However, little is known about the interactions of acids and amines on such surfaces. We report here infrared spectroscopy studies of the uptake and reaction of gaseous TMA with MSA on silicon powders both in the absence and presence of water vapor. On the basis of these studies, this heterogeneous chemistry could explain the difficulty in efficiently and accurately sampling and analyzing amines in air, and conversely MSA, and also have a potential impact on amine concentrations in the boundary layer.

EXPERIMENTAL SECTION

Diffuse reflectance infrared Fourier transform spectrometry (DRIFTS) experiments were conducted at 296 ± 1 K in a flow

Received: August 29, 2013
Revised: December 2, 2013
Accepted: December 4, 2013
Published: December 4, 2013

system using a Harrick Scientific vacuum reaction cell (model HVC-DR2) equipped with a diffuse reflectance attachment (model DRA-2CS) situated in a sampling compartment of a Fourier transform infrared spectrometer (Mattson, RS 10000, now Thermo Electron Corp., Madison, WI). The interior walls of the cell and ZnSe windows were coated with halocarbon wax (Halocarbon Products Corporation, River Edge, NJ) to prevent corrosion by MSA. A detailed description of the DRIFTS apparatus can be found elsewhere.[45,46] Briefly, the reaction cell had an internal sample cup (1.1 cm in diameter and 0.3 cm in depth) into which 0.3 g of silicon (Si) powder (60 mesh, 99.999% trace metal basis, Sigma-Aldrich, used as received) was tightly pressed. The Brunauer−Emmett−Teller (BET) surface area of silicon powder was measured using nitrogen adsorption with an Autosorb-1 Surface Area Analyzer (Quantachrome Instruments, Boynton Beach, FL) to be 7.0 ± 0.6 m^2 g^{-1} (1σ). Gases entered the cell from an inlet port at the side of the cell and were pumped at ∼450 mL min^{-1} through the sample, exiting through an outlet port at the side of the sample cup, with the residence time in the reaction cell of ∼1.5 s. Prior to experiments, the reaction cell with the silicon powder in the sampling cup was purged overnight with dry synthetic air (Ultra Zero grade air, H_2O < 2 ppm, CO < 0.05 ppm, THC < 0.05 ppm, NO_x < 0.02 ppm, PRAXAIR Inc., Danbury, CT) to remove water, although small amounts of adsorbed water are still expected to remain on the surface. ZnSe windows allow transmission of the IR beam to the solid sample where diffuse reflectance occurs. However, strong absorptions by the halocarbon wax on ZnSe windows were observed in the 900−1000 cm^{-1} wavenumber region, and thus this region was not used for analyses. The single beam DRIFTS spectra before, during, and after the reaction were collected by averaging 512 scans at 2 cm^{-1} resolution.

Gas-phase MSA was generated by passing dry air over pure liquid MSA (99.0%; Sigma-Aldrich). The concentration of MSA in the gas stream was not measured but based on other studies in this laboratory, it is approximately 200 ppb. Gas-phase TMA obtained as a 1 ppm mixture in N_2 (Airgas, Radnor, PA) was used as received. The silicon powder was conditioned with gaseous MSA for 1−1.5 days. This lengthy conditioning process was required because MSA was readily taken up on other surfaces (e.g., tubing and the reaction cell walls) prior to contacting the silicon and its concentration in the gas phase only slowly approaches a steady state. Subsequently, the TMA exposure was conducted for 30 min or 1 h at 450 mL min^{-1} in all experiments. Gas-phase TMA concentrations were measured at the inlet of an MSA-conditioned DRIFTS cell and at the outlet in the absence of silicon powder by collecting the gas flow on a cartridge packed with a weak cation exchange resin and then extracting the resin and analyzing the extract by ion chromatography.[47] Humidified air was generated by passing air through a bubbler containing purified water (Milli-Q Plus, 18.2 MΩ cm) and diluted with dry air to achieve 10% relative humidity (RH).

For comparison to the TMA reaction, the MSA-coated silicon powder was exposed to gaseous NH_3 in separate experiments. Ammonia was generated by passing dry air over ammonium hydroxide (ammonia in water, 28.71 wt %, certified ACS Plus, Thermo Fisher Scientific Inc.) that would give ∼550 Torr partial pressure of NH_3 at 296 ± 1 K.[48] Gas-phase ammonia was measured using the same technique as for TMA described above.

Trimethylaminium methanesulfonate salt was prepared by mixing equal moles of MSA and TMA (45 wt % in H_2O, Sigma-Aldrich) in aqueous solution. A small amount of solution was placed onto a 2.5 cm ZnSe window using a Q-tip soaked with the solution and then dried in an air-purged IR compartment. The single beam spectra of a clean window and the window with adsorbed salts were collected in transmission mode by averaging 32 scans at a resolution of 2 cm^{-1}.

RESULTS AND DISCUSSION

Silicon powder was used in these studies for a number of reasons. First, it has an oxide layer on its surface, so that it is a reasonable model for some boundary-layer building materials where silicon oxides are common components[42] Second, silicon powder is infrared transparent over most of the spectral regions of interest (with the exception of the 900−1000 and 1100−1300 cm^{-1} regions). The third important property is that the surface itself is expected to be less reactive than many other DRIFTS substrates to strong acids such as MSA because it is coated with a thin layer of SiO_x formed by air oxidation.[49,50] This oxide layer has been shown to increase in thickness as the silcon powder is heated in air, but focused ion beam-scanning electron microscope (FIB-SEM) images show that even for thick SiO_x layers, the coating is quite irregular with obvious pores and defects.[50] Thus, although most of the surface is coated with SiO_x, some of the underlying silicon remains accessible to gases.

Figure 1a,b shows representative changes in the DRIFTS spectra of silicon powder upon exposure to either gaseous (a) MSA or (b) TMA, respectively. Spectra (A = log S_0/S_1) are obtained by taking the ratio of the spectrum scanned during the MSA or TMA exposure (S_1) to the spectrum before the exposure (S_0). Thus, the changes shown are due to the uptake and/or reaction of MSA or TMA, with positive peaks representing new or increased absorptions and negative peaks representing losses compared to the silicon powder alone. In the case of exposure to MSA (Figure 1a), the most prominent change is a new peak at 1362 cm^{-1} attributable to the asymmetric stretch of S(O)(O).[51−53] A small peak at 3036 cm^{-1} results from the stretch of OH of MSA, ν(OH).[51,53] The negative peak at 3743 cm^{-1} is due to a decrease in the free O−H on the surface,[54−56] which can occur due either to hydrogen bonding with a species such as MSA, or to reaction. When the silicon surface was purged with dry air after the MSA exposure, the peak at 1362 cm^{-1} decreases, while the negative peak at 3743 cm^{-1} remains. This suggests that the species associated with the 1362 cm^{-1} peak desorbs relatively easily from the surface, and is independent of the species causing the change in the surface O−H. We assign this peak at 1362 cm^{-1} to surface-adsorbed molecular MSA. The peak at 3743 cm^{-1} due to surface O−H on silicon powder is also negative when the surface is exposed to water vapor alone, due to hydrogen bonding of the surface free O−H to water. However, this is reversible, with the 3743 cm^{-1} peak recovering upon removal of the water in a stream of dry gas. This comparison suggests that during the MSA exposure, the surface free O−H reacts/interacts with a species that is strongly bound and is not readily removed from the surface. We assign this species to the $CH_3SO_3^-$ anion from MSA dissociation. There is a small shoulder at 1342 cm^{-1} (shown in the inset of Figure 1a) which based on spectra of the salt (see below) is assigned to the asymmetric stretch of S(O)(O) in the anion. The broad

dx.doi.org/10.1021/es403845b | Environ. Sci. Technol. 2014, 48, 323−330

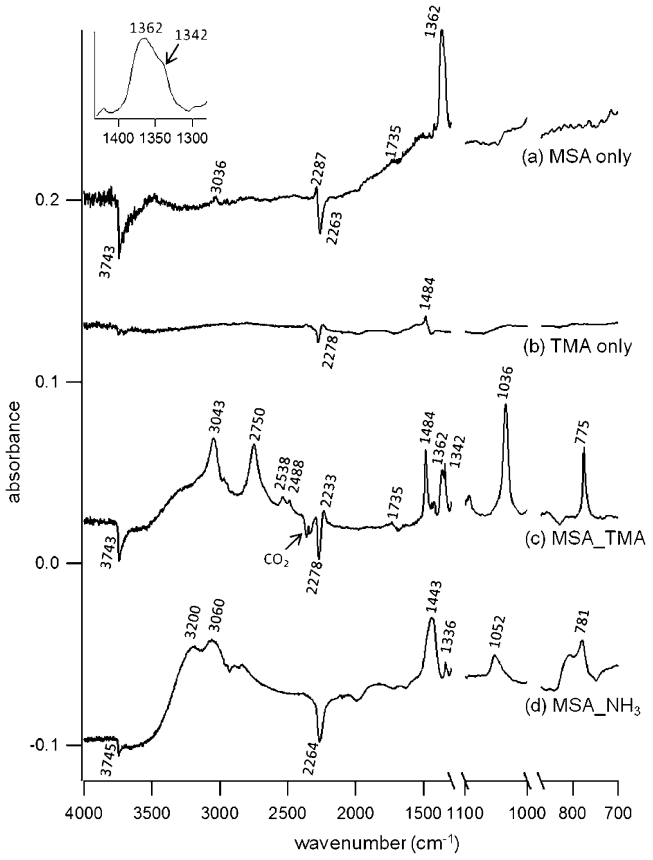

Figure 1. Changes in the absorption spectra (A = log S_0/S_1) of Si powder due to (a) MSA exposure in air and (b) TMA exposure in N_2, where S_0 is the single beam spectrum taken before the MSA or TMA exposure and S_1 is that during the MSA or TMA exposure; (c) MSA and then TMA exposure and (d) MSA and then NH_3 exposure, where S_0 is the single beam spectrum taken before MSA and TMA or NH_3 exposure and S_1 is that taken when the Si surface is exposed to MSA first and then to TMA or NH_3. Spectra are offset from their normal baselines for clarity. The inset on the top left shows the enlarged spectrum of (a) over the region 1300−1450 cm^{-1}.

shoulder around 1735 cm^{-1} may be due to H_3O^+,[57−59] which has also been seen with nitric acid on surfaces.[60]

Changes in the peaks in the 2200−2300 cm^{-1} region are attributed to changes in absorptions of the silicon substrate. While the specific functional groups responsible for these changes are not clear, the Si−H bond has stretching vibrations in this region, with their exact position dependent on the environment around the Si as well as the nature of a solid surface (e.g., amorphous or crystalline).[61−63] For example, the peak shifts to higher frequencies when Si is surrounded by atoms with a higher electronegativity than Si such as an oxygen atom.[61,63] Thus, the stretch of O_3Si−H on SiO_2 is found in the range from 2260 to 2280 cm^{-1}, while Si_3Si−H can be detected at 1995 cm^{-1} (see below and Figure 4a). Small changes in this region indicate that some of the underlying silicon substrate is accessible to the MSA.

The exposure of the silicon surface to TMA alone (Figure 1b) results in a small peak at 1484 cm^{-1}, assigned to the asymmetric bend of the $-CH_3$ group.[64] However, when a surface that was first exposed to MSA is subsequently exposed to TMA, large changes occur in the spectrum (Figure 1c). First, the peak observed from MSA at 1362 cm^{-1} decreases upon TMA exposure, and the peak from TMA at 1484 cm^{-1} increases significantly compared to the case for exposure of the silicon powder to TMA alone for the same amount of time. New positive peaks are also observed at 775, 1036, 2750, and 3043 cm^{-1}, with smaller peaks at 2488 and 2538 cm^{-1}. The peak at 1342 cm^{-1} previously assigned to the $CH_3SO_3^-$ anion is much stronger now.

Figure 2 shows relative intensities of the major product peaks, normalized to the final point of each peak, as a function

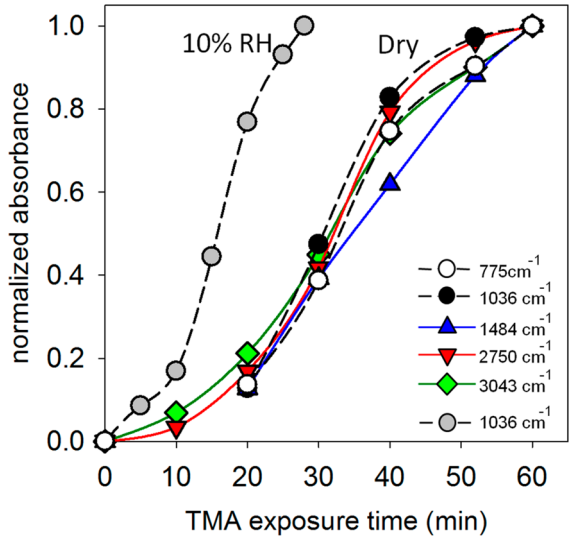

Figure 2. Relative intensities of major peaks formed in the reaction of MSA with gaseous TMA on Si powder as a function of TMA exposure time. Peaks at each time were normalized to the final point for that peak at 60 min for dry and at 28 min for humid conditions. The initial induction period is due to conditioning of the sampling lines and reaction cell after the flow of TMA is initiated.

of the TMA exposure time (the peak at 1342 cm^{-1} is not included because the strong overlap with the 1362 cm^{-1} peak precludes separating its contribution). Note that there is ∼10−15 min induction time where growth of new peaks is slow. This is attributed to the "stickiness" of TMA that is easily lost on surfaces in the system (e.g., tubing, surfaces of the reaction cell) before it reaches the MSA-coated silicon powder. The time dependence of the growth of each of these new peaks (under dry conditions) is similar, suggesting that either they are attributable to the same species or they are different species but formed simultaneously. Using literature data for mixtures of MSA and diethylamine in the liquid-phase,[53] of alkanesulfonic acids, esters and salts,[65] and of methyl methanesulfonate in the liquid and solid states,[66] these peaks were tentatively assigned as follows: 775 cm^{-1}, ν(C−S) or ν(S−O);[67] 1036 cm^{-1}, ν_s((S(O)(O)); 2750 and 3043 cm^{-1}, ν(CH).

For comparison, an absorption spectrum of synthesized trimethylaminium methanesulfonate salt [$CH_3SO_3^-\cdot(CH_3)_3NH^+$] deposited on a ZnSe window is shown in Figure 3. It is clear that the peaks due to the salt are essentially the same as those in the DRIFTS spectra of the silicon surface exposed to gaseous MSA and then to gaseous TMA (see Figure 1c), establishing that the MSA−amine reaction on the surface forms the trimethylaminium methanesulfonate salt. In the transmission spectrum of the salt, there are also a number of strong peaks in the 900−1300 cm^{-1} region which are similar to those reported in a liquid mixture of MSA with diethylamine[53] but which are not accessible in the DRIFTS studies because of

dx.doi.org/10.1021/es403845b | Environ. Sci. Technol. 2014, 48, 323−330

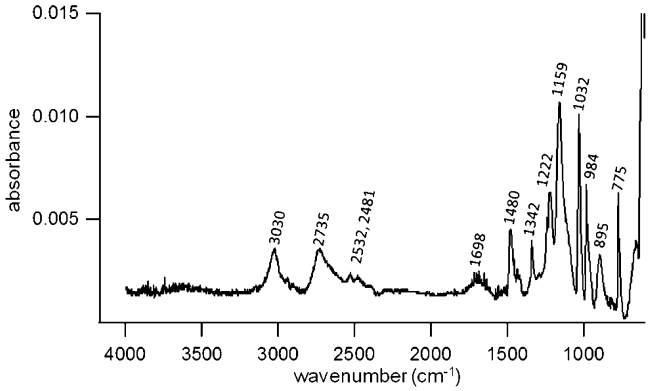

Figure 3. Absorption spectrum (A = log S_0/S_1) of trimethylaminium methanesulfonate salt on a ZnSe window, where S_0 is the single beam spectrum of the clean ZnSe window and S_1 is that with the salt on the ZnSe.

the strong absorptions by the silicon substrate and halocarbon wax on the ZnSe windows. The presence of the peak at 1362 cm^{-1} in the MSA spectrum (Figure 1a) but not in the salt spectrum (Figure 3) supports the previous assignment of the 1362 cm^{-1} peak to undissociated molecular MSA and the 1342 cm^{-1} peak to the $CH_3SO_3^-$ anion.

There is a possibility of other surface reactions occurring during the experiments. Reactions that occur slowly in the gas phase often occur much more readily on surfaces.[68] One potential reaction of MSA with TMA is the conversion of TMA to ammonia and MSA to its methyl ester:

$$3CH_3S(O)(O)OH + (CH_3)_3N \rightarrow NH_3 + 3CH_3S(O)(O)OCH_3 \quad (1)$$

Generation of gas-phase NH_3 has been reported when ammonium salts were exposed to gas-phase amines as a result of a displacement reaction of ammonium ions by aminium ions.[36,37,69] If reaction 1 occurred, the methyl ester should be observed in DRIFTS spectra. However, spectra of the ester (liquid and solid)[66] are similar to that of reactant MSA, and they are not readily distinguished from each other. If NH_3 were formed it could react with MSA on the surface. Figure 1d shows changes in the absorption spectrum when the silicon surface that was first exposed to MSA is subsequently exposed to NH_3. As for Figure 1c, the spectrum (S_1) in Figure 1d is ratioed to the spectrum taken before the MSA exposure (S_0), so the absorption spectrum (A = log S_0/S_1) represents net changes from the bare silicon substrate. Similar to observations in the MSA plus TMA exposure, the −S(O)(O)− peak at 1362 cm^{-1} assigned to molecular MSA decreases upon exposure to ammonia, while other new peaks appear. Peaks at 3060 and 3200 cm^{-1} are assigned to the deformation and asymmetric stretch of NH_4^+, and the peak at 1443 cm^{-1} is assigned to asymmetric deformation of NH_4^+.[70,71] Peaks at 781 and 1336 cm^{-1} are similar to the peaks observed in the MSA−TMA experiments at 775 and 1342 cm^{-1}, assigned to ν(C−S) or ν(S−O)[67] and the asymmetric stretch of S(O)(O) in the $CH_3SO_3^-$ anion, respectively (see Figure 1c). The loss of the MSA peak at 1362 cm^{-1} and the formation of peaks due to NH_4^+ shows that the MSA reacts with NH_3, forming ammonium methanesulfonate salt on the surface. The lack of formation of the characteristic ammonium salt peaks in the MSA−TMA spectrum (Figure 1c) suggests that the conversion of TMA to NH_3 and its subsequent reaction with MSA on the surface is not important.

However, if reaction 1 occurred and the NH_3 was pumped out before reacting with MSA on the surface, the ammonium salt would not be observed and instead, gas-phase NH_3 would have been formed. Therefore, a search was also made for NH_3 in the gas phase. Gas-phase ammonia was measured at the outlet of the DRIFTS cell after the MSA conditioned silicon powder was exposed to TMA. Additional non-DRIFTS experiments were conducted using high surface area materials to increase the potential amount of ammonia formed. Either silica gel or glass wool in a quartz tube was conditioned with MSA, and then TMA was introduced as in the DRIFTS experiments. The formation of gas-phase ammonia was negligible within experimental error, supporting the conclusion from the DRIFTS experiments that reaction 1 does not occur on surfaces.

Experiments with TMA and MSA were also conducted in the presence of water vapor. After the MSA exposure, the silicon powder was exposed to water vapor at 10% RH for 1 h and then to gaseous TMA, with the RH maintained at 10% during the TMA exposure. Figure 4a,c shows changes in the absorption spectra when the silicon surface initially conditioned

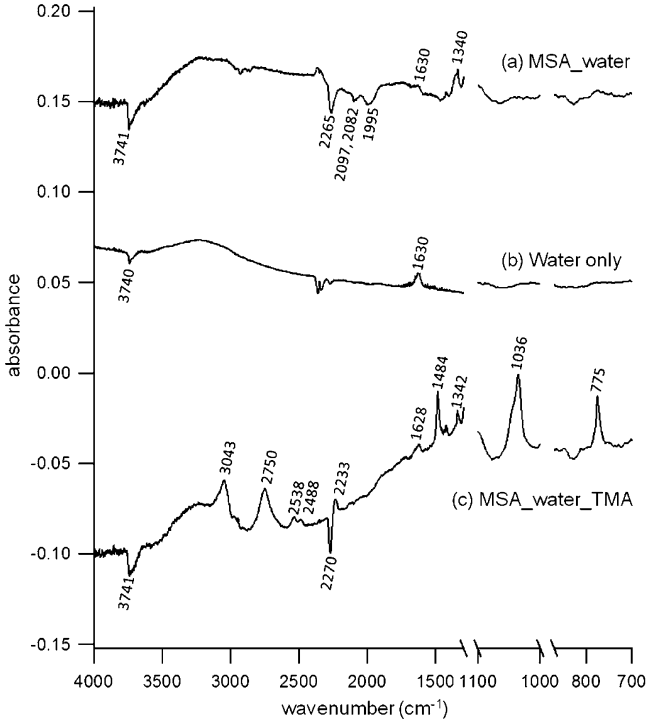

Figure 4. Changes in the absorption spectra (A = log S_0/S_1) of Si powder due to (a) MSA and then water (10% RH) exposures, where S_0 is the single beam spectrum taken before MSA exposure and S_1 is that taken when the Si surface is exposed to MSA first and then to water vapor; (b) water vapor (10% RH) exposure, where S_0 is the single beam spectrum taken before water vapor exposure and S_1 is that taken when the surface is exposed to water vapor; (c) MSA, water vapor (10% RH), and then TMA exposure, where S_0 is the single beam spectrum taken before MSA exposure and S_1 is that when the Si surface is exposed to MSA first, water vapor second, and then TMA. In addition to surface adsorbed water, peaks due to gaseous water vapor inside the DRIFTS reaction cell were also seen and were subtracted from all spectra. Spectra are offset from their normal baselines for clarity.

dx.doi.org/10.1021/es403845b | Environ. Sci. Technol. 2014, 48, 323−330

by MSA is exposed to (a) water vapor and then to (c) gaseous TMA. The spectra (S_1) are ratioed to the spectrum taken before the MSA exposure (S_0), so these spectra ($A = \log S_0/S_1$) represent net changes from the bare silicon substrate. Absorption due to gas-phase water vapor inside the reaction cell was subtracted from the absorption spectra so the change due to MSA and TMA could be more readily seen. Figure 4a shows that when the MSA-conditioned silicon surface is exposed to water vapor, the peak at 1362 cm^{-1} assigned to molecular MSA (Figure 1a) is not evident but the peak at ~1340 cm^{-1} assigned to the $CH_3SO_3^-$ anion is clearly seen.

Peaks due to the stretching and bending mode of H_2O as seen for the silicon surface exposed to water vapor alone (Figure 4b) are observed at 3000−3400 cm^{-1} and 1630 cm^{-1}, respectively.[72−74] Peaks in the 1900−2300 cm^{-1} region due to substrate Si−H decrease as in the absence of water vapor (Figure 1a), with that at 1995 cm^{-1} assigned to Si_3Si-H decreasing relatively more when both MSA and water are present (Figure 4a). When the surface is exposed to water vapor alone, these peaks decrease but to such a small extent that they are not readily seen in Figure 4b. Therefore, the decrease seen in Figure 4a is due to the exposure to both MSA and water vapor. The oxidation of silicon powder by O_2 is known to be accelerated in the presence of water[49,50] and one possibility is that this is accelerated even more in the presence of MSA. This would permanently change the IR spectrum. However, when TMA is added, this negative peak at 1995 cm^{-1} is no longer seen (Figure 4c), suggesting that the change seen with MSA and water is reversible. It may be that the proton liberated by dissociation of MSA in the presence of water is responsible for the change in the Si−H stretch but is transferred to the basic amine when TMA is added. Other than this, the absorption spectrum when gaseous TMA is added to the system in the presence of water vapor (Figure 4c) is similar to the spectrum in its absence (Figure 1c), i.e, the trimethylaminium methanesulfonate salt is formed from the MSA + TMA reaction on the surface both in the presence and absence of water. Note that, as shown in Figure 2, the salt formation is faster under humid conditions. The absorption peaks due to the salt are not changed when the silicon surface is dried for ~3 h, suggesting that the salt product is nonvolatile.

In short, we have established that surface-bound MSA reacts with gaseous TMA both in the presence and absence of water vapor. In the presence of water, the MSA is dissociated prior to the addition of TMA, while under dry conditions some remains in the undissociated molecular form. However, in either case, the reaction leads to the formation of trimethylaminium methanesulfonate salt on the surface. While the present study began with MSA on the surface and then gas-phase TMA being added, similar chemistry would be expected if the amine was on the surface and then gas-phase MSA was added, which would represent an additional loss process for gas-phase MSA. One would expect similar chemistry to occur between sulfuric acid deposited on a surface and amines. Although there are no directly related studies with which to compare the present results, the heterogeneous uptake of gaseous alkylamines on a sulfuric acid aqueous solution has been shown to be an irreversible reaction, supporting the formation of nonvolatile salts.[75]

In the troposphere, MSA is formed by the oxidation of organosulfur compounds.[12] Its major fate is uptake into existing particles, reaction with amines to form new particles,[28] and deposition. In the boundary layer where surfaces are plentiful, deposition is likely to be significant. Both MSA and amines reversibly adsorb on surfaces, and after uptake, can desorb either through a reduction in their gas-phase concentration or by a competitive displacement mechanism. The current studies show that uptake of one of these species onto a surface holding the second reactant leads to the formation of an nonvolatile salt, that is, to irreversible uptake of the gas. Although our studies focused on MSA, a similar process is likely to apply to sulfuric acid which is typically a copollutant with MSA.

An estimate of the lower limit to the uptake coefficient for TMA on the MSA-coated silicon powder was obtained from the increase in the 1036 cm^{-1} peak with time. For quantification of product formation, a known concentration of MSA−TMA salt aqueous solution was mixed with a known mass of silicon powder, and the water evaporated. The known concentration of MSA−TMA salt mixed with this powder was used along with its DRIFTS spectrum to relate peak intensity to the effective salt surface concentration (molecules cm^{-2}). Using the linear portion of the time dependence for salt formation from 20 to 30 min (Figure 2), the initial growth of the salt is 1.9×10^{10} salt molecules cm^{-2} s^{-1}. This represents the rate of product formation which is given by γ [TMA]$(RT/(2\pi M))^{0.5}$, where γ is the reaction probability, [TMA] is the gas phase concentration of the amine, R is the gas constant, T is the temperature, and M the molecular mass of TMA. Although the concentration of TMA used in these experiments was nominally 1 ppm, the concentration reaching the MSA-coated silicon powder that is being spectroscopically interrogated is expected to be significantly smaller because of the uptake of TMA on the inlet lines and the walls of the reaction chamber. This loss was determined to be 80% of the initial concentration by measuring the average TMA over the exposure time from 20 to 60 min (Figure 2) at the inlet and outlet of the MSA-conditioned DRIFTS cell in the absence of the silicon powder. The effective average TMA concentration to which the MSA on the silicon powder was exposed over 20−60 min exposure time was thus only 0.2 ppm. Using this concentration, the value of γ is 5×10^{-7} under dry conditions. However, water vapor is always present in the troposphere, and as seen in Figure 2, the rate of salt formation is about a factor of 2 faster with water even at the relatively low concentration corresponding to 10% RH. Thus, the atmospherically relevant *lower limit* value derived for γ from these experiments is $\sim 10^{-6}$.

This approach will underestimate the reaction probability for a number of reasons. First, this calculation assumes that the signals from the salt-silicon mixture are representative of salts formed *in situ* from the MSA−TMA reaction. In reality, uneven pumping of TMA through the salt sample likely results in the area that is interrogated spectroscopically during the reaction being less than sampled for the calibration salt−silicon powder mixture. In addition, the distribution of the salt in the silicon powder will be relatively homogeneous for the calibration mixture compared to that from the MSA + TMA reaction, where salt formation at the very top layers where TMA first impacts the sample will dominate. Second, the effective TMA concentration is assumed to be constant at 0.2 ppm. However, this is the average concentration, while the actual concentration likely increases with time as the surface is conditioned with TMA. As a result, the actual TMA over the 20−30 min linear part of the curve in Figure 2 used to obtain γ is likely smaller than 0.2 ppm, which would increase the derived value of γ. Adsorbed MSA on the silicon powder surface available for the reaction was also assumed to be constant, while it will be

decreasing with increasing TMA exposure time. For example, if the data at 60 min reaction time in Figure 2 are taken to represent full reaction of the available MSA, then the MSA remaining in the linear region used to derive a value for γ is ~50% of the initial MSA, which would increase the estimated reaction probability by a factor of 2.

We note that the uptake coefficients for TMA on ammonium salts (where exchange reactions that displace ammonia occur) such as $(NH_4)_2SO_4$ under dry conditions[69] and on NH_4NO_3 at 20% RH[36] have been measured to be 2×10^{-4} and 2×10^{-3}, respectively. It is reasonable to expect that the acid−base reaction would be at least as fast as the exchange reaction, suggesting that the true value of the reaction probability for TMA with surface-bound MSA is likely at least two to three orders of magnitude greater than our lower limit.

These studies have implications for the sampling of MSA and amines. Both are notoriously difficult to measure due to uptake on sampling surfaces and inlets. With the relatively recent recognition of the importance of amines in new particle formation,[21,22,25,27,35,39] there has been more effort placed on measuring their gas-phase concentrations.[76−80] This has proven challenging not due to the lack of analytical approaches, but rather to uptake of the amines on sampling lines and inlets. In studies in this laboratory even in the absence of acids, competitive adsorption of TMA onto sampling lines made of Teflon, glass, and stainless steel has been observed; once lines have been used for TMA and then flushed with synthetic air, the addition of a different amine displaces TMA back into the gas phase. A similar competitive adsorption has been observed for PEEK tubing. Thus the reported concentrations of amines in air may in many cases represent a lower limit.

In the atmosphere where sampling lines are exposed to many different species including sulfuric acid and MSA, irreversible uptake of the amine seems likely based on the present studies. The first order rate constant for loss of TMA to the surface (k) is given by $k = \gamma(S/V)(RT/(2\pi M))^{0.5}$, where S/V is the surface-to-volume ratio, R is the gas constant, T is the temperature, and M is the molecular mass. The lifetime (τ) with respect to reaction at the surface is given by $\tau = 1/k$. As an example, the lifetime of TMA in a typical 3 m long 2″ i.d. sampling line[81] that is conditioned with MSA is estimated to be 150 s using $\gamma = 10^{-6}$. However, given that this is a lower limit and the actual value may well be at least two to three orders of magnitude faster, the lifetime of TMA in the sampling line is likely of the order of seconds or less. At a sampling rate through the line of 63 L min^{-1},[81] the residence time of TMA is ~6 s, suggesting there is sufficient time for significant loss of the amine in the sampling line. If the uptake of amines follows the same trend[69] as reported for uptake and reaction with $(NH_4)_2SO_4$, the loss of methylamine and dimethylamine could be even more significant.

The surface reaction described here could also impact amine concentrations in air. For example, the UCI-CIT airshed model[82,83] has five layers in the vertical direction, with the height of the first one representing the boundary layer being 38 m. The lifetime of TMA by deposition onto acid-conditioned surfaces is estimated to be ~130 h for $\gamma = 10^{-6}$, but only ~1.3 h at $\gamma = 10^{-4}$ and ~8 min at $\gamma = 10^{-3}$. This can be compared to other loss processes for gas-phase amines. TMA reacts with OH radicals[84] and ozone,[85] with rate constants of 6.1×10^{-11} and 7.8×10^{-18} cm^3 $molecules^{-1}$ s^{-1}, respectively. Assuming that concentrations of OH radicals and ozone are 10^6 and 2.5×10^{12} molecules cm^{-3}, respectively, then the lifetime of TMA is 4.6 h for the OH radical reaction and 14 h for the ozone reaction. Amines also react with sulfuric acid or MSA to form clusters during the new particle formation process. Assuming the concentration of acid to be 10^6 molecules cm^{-3} and the cluster formation rate constant to be 10^{-10} cm^3 $molecule^{-1}$ s^{-1}, then the lifetime of TMA is 2.8 h. Thus, the surface loss in the boundary layer may be significant compared to other loss processes, particularly at night when concentrations of OH radical and ozone are low.

AUTHOR INFORMATION

Corresponding Author

*Phone: 949-824-7670; fax: 949-824-2420; e-mail: bjfinlay@uci.edu.

Notes

The authors declare no competing financial interest.

ACKNOWLEDGMENTS

We are grateful for funding from the National Science Foundation (Grant No. 0909227) and the Department of Energy (Grant No. ER65208). We would like to thank Professor Kenneth J. Shea and Professor Zhibin Guan for access to the Autosorb-1 Surface Area Analyzer. We are also grateful to Professor James N. Pitts Jr. for helpful discussions and comments on the manuscript.

REFERENCES

(1) Aneja, V. P. Natural sulfur emissions into the atmosphere. *J. Air Waste Manage. Assoc.* **1990**, *40*, 469−476.

(2) Bates, T. S.; Lamb, B. K.; Guenther, A.; Dignon, J.; Stoiber, R. E. Sulfur emissions to the atmosphere from natural sources. *J. Atmos. Chem.* **1992**, *14*, 315−337.

(3) Bentley, R.; Chasteen, T. G. Environmental VOSCs—Formation and degradation of dimethyl sulfide, methanethiol and related materials. *Chemosphere* **2004**, *55*, 291−317.

(4) Williams, J.; Wang, N. Y.; Cicerone, R. J.; Yagi, K.; Kurihara, M.; Terada, F. Atmospheric methyl halids and dimethyl sulfide from cattle. *Geophys. Res. Lett.* **1999**, *13*, 485−491.

(5) Sato, H.; Hirose, T.; Kimura, T.; Moriyama, Y.; Nakashima, Y. Analysis of malodorous volatile substances of human waste: Feces and urine. *J. Health Sci.* **2001**, *47*, 483−490.

(6) Rosenfeld, P. E.; Henry, C. L.; Dills, R. L.; Harrison, R. B. Comparison of odor emissions from three different biosolids applied to forest soil. *Water Air Soil Pollut.* **2001**, *127*, 173−191.

(7) Vassilakos, C.; Papadopoulos, A.; Lahaniati, M.; Maggos, T.; Bartzis, J.; Papagianakopoulos, P. Measurements of sulfur pollutants and VOC concentrations in the atmosphere of a suburban area in Greece. *Fresenius Environ. Bull.* **2002**, *11*, 516−521.

(8) Meinardi, S.; Simpson, I. J.; Blake, N. J.; Blake, D. R.; Rowland, F. S. Dimethyl disulfide (DMDS) and dimethyl sulfide (DMS) emissions from biomass burning in Australia. *Geophys. Res. Lett.* **2003**, *30*, No. 1454.

(9) Correa, S. M.; Arbilla, G. Mercaptans emissions in diesel and biodiesel exhaust. *Atmos. Environ.* **2008**, *42*, 6721−6725.

(10) Aneja, V. P.; Schlesinger, W. H.; Erisman, J. W. Effects of agriculture upon the air quality and climate: research, policy, and regulations. *Environ. Sci. Technol.* **2009**, *43*, 4234−4240.

(11) Yokelson, R. J.; Crounse, J. D.; DeCarlo, P. F.; Karl, T.; Urbanski, S.; Atlas, E.; Campos, T.; Shinozuka, Y.; Kapustin, V.; Clarke, A. D.; Weinheimer, A.; Knapp, D. J.; Montzka, D. D.; Holloway, J.; Weibring, P.; Flocke, F.; Zheng, W.; Toohey, D.; Wennberg, P. O.; Wiedinmyer, C.; Mauldin, L.; Fried, A.; Richter, D.; Walega, J.; Jimenez, J. L.; Adachi, K.; Buseck, P. R.; Hall, S. R.; Shetter, R. Emissions from biomass burning in the Yucatan. *Atmos. Chem. Phys.* **2009**, *9*, 5785−5812.

(12) Finlayson-Pitts, B. J.; Pitts, J. N., Jr. *Chemistry of the Upper and Lower Atmosphere—Theory, Experiments, and Applications*; Academic Press: San Diego, 2000; p 969.
(13) Berresheim, H.; Eisele, F. L.; Tanner, D. J.; McInnes, L. M.; Ramseybell, D. C.; Covert, D. S. Atmospheric sulfur chemistry and cloud condensation nuclei (CCN) concentrations over the northeastern Pacific Coast. *J. Geophys. Res.* **1993**, *98*, 12701−12711.
(14) Eisele, F. L.; Tanner, D. J. Measurement of the gas phase concentration of H_2SO_4 and methane sulfonic acid and estimates of H_2SO_4 production and loss in the atmosphere. *J. Geophys. Res.* **1993**, *98*, 9001−9010.
(15) Jefferson, A.; Tanner, D. J.; Eisele, F. L.; Berresheim, H. Sources and sinks of H_2SO_4 in the remote Antarctic marine boundary layer. *J. Geophys. Res.* **1998**, *103*, 1639−1645.
(16) Jefferson, A.; Tanner, D. J.; Eisele, F. L.; Davis, D. D.; Chen, G.; Crawford, J.; Huey, J. W.; Torres, A. L.; Berresheim, H. OH photochemistry and methane sulfonic acid formation in the coastal Antarctic boundary layer. *J. Geophys. Res.* **1998**, *103*, 1647−1656.
(17) Mauldin, R. L., III; Tanner, D. J.; Heath, J. A.; Huebert, B. J.; Eisele, F. L. Observations of H_2SO_4 and MSA during PEM-Tropics-A. *J. Geophys. Res.* **1999**, *104*, 5801−5816.
(18) Mauldin, R. L., III; Cantrell, C. A.; Zondlo, M. A.; Kosciuch, E.; Ridley, B. A. Measurements of OH, H_2SO_4 and MSA during tropospheric ozone production about the spring equinox (TOPSE). *J. Geophys. Res.* **2003**, *108*, DOI: 10.1029/2002JD002295.
(19) Benson, D. R.; Erupe, M. E.; Lee, S.-H. Laboratory-measured H_2SO_4−H_2O−NH_3 ternary homogeneous nucleation rates: Initial observations. *Geophys. Res. Lett.* **2009**, *36*, L15818.
(20) Wang, L.; Khalizov, A. F.; Zheng, J.; Xu, W.; Ma, Y.; Lal, V.; Zhang, R. Atmospheric nanoparticles formed from heterogeneous reactions of organics. *Nat. Geosci.* **2010**, *3*, 238−242.
(21) Smith, J. N.; Barsanti, K. C.; Friedli, H. R.; Ehn, M.; Kulmala, M.; Collins, D. R.; Scheckman, J. H.; Williams, B. J.; McMurry, P. H. Observations of aminium salts in atmospheric nanoparticles and possible climatic implications. *Proc. Natl. Acad. Sci. U.S.A.* **2010**, *107*, 6634−6639.
(22) Erupe, M. E.; Viggiano, A. A.; Lee, S.-H. The effect of trimethylamine on atmospheric nucleation involving H_2SO_4. *Atmos. Chem. Phys.* **2011**, *11*, 4767−4775.
(23) Kirkby, J.; Curtius, J.; Almeida, J.; Dunne, E.; Duplissy, J.; Ehrhart, S.; Franchin, A.; Gagné, S.; Ickes, L.; et al. Role of sulphuric acid, ammonia and galactic cosmic rays in atmospheric aerosol nucleation. *Nature* **2011**, *476*, 429−433.
(24) Chen, M.; Titcombe, M.; Jiang, J.; Jen, C.; Kuang, C.; Fischer, M. L.; Eisele, F. L.; Siepmann, J. I.; Hanson, D. R.; Zhao, J.; McMurry, P. H. Acid-base chemical reaction model for nucleation rates in the polluted atmospheric boundary layer. *Proc. Natl. Acad. Sci. U.S.A.* **2012**, *109*, 18713−18718.
(25) Zollner, J. H.; Glasoe, W. A.; Panta, B.; Carlson, K. K.; McMurry, P. H.; Hanson, D. R. Sulfuric acid nucleation: power dependencies, variation with relative humidity, and effect of bases. *Atmos. Chem. Phys.* **2012**, *12*, 4399−4411.
(26) Kulmala, M.; Kontkanen, J.; Junninen, H.; Lehtipalo, K.; Manninen, H. E.; Nieminen, T.; Petäjä, T.; Sipilä, M.; Schobesberger, S.; Rantala, P.; et al. Direct observations of atmospheric aerosol nucleation. *Science* **2013**, *339*, 943−946.
(27) Qiu, C.; Zhang, R. Multiphase chemistry of atmospheric amines. *Phys. Chem. Chem. Phys.* **2013**, *15*, 5738−5752.
(28) Dawson, M. L.; Varner, M. E.; Perraud, V.; Ezell, M. J.; Gerber, R. B.; Finlayson-Pitts, B. J. Simplified mechanism for new particle formation from methanesulfonic acid, amines and water via experiments and *ab initio* calculations. *Proc. Natl. Acad. Sci. U.S.A.* **2012**, *109*, 18719−18724.
(29) Hinds, W. C. *Aerosol technology: properties, behavior and measurement of airborne particles*; John Wiley & Sons Inc.: New York, 1999.
(30) Dockery, D. W.; Pope, C. A.; Xu, X. P.; Spengler, J. D.; Ware, J. H.; Fay, M. E.; Ferris, B. G.; Speizer, F. E. An association between air-pollution and mortality in six United States cities. *New Engl. J. Med.* **1993**, *329*, 1753−1759.
(31) Pope, C. A.; Dockery, D. W. Health effects of fine particulate air pollution: Lines that connect. *J. Air Waste Manage. Assoc.* **2006**, *56*, 709−742.
(32) Mauderly, J. L.; Chow, J. C. Health effects of organic aerosols. *Inhal. Toxicol.* **2008**, *20*, 257−288.
(33) *IPCC Climate change 2007: Synthesis report*; Contribution of working groups I, II, and III to the fourth assessment report of the intergovernmental panel on climate change. IPCC: Geneva, Switzerland, 2007.
(34) Cape, J. N.; Cornell, S. E.; Jickells, T. D.; Nemitz, E. Organic nitrogen in the atmosphere—Where does it come from? A review of sources and methods. *Atmos. Res.* **2011**, *102*, 30−48.
(35) Ge, X.; Wexler, A. S.; Clegg, S. L. Atmospheric amines—Part I. A review. *Atmos. Environ.* **2011**, *45*, 524−546.
(36) Lloyd, J. A.; Heaton, K. J.; Johnston, M. V. Reactive uptake of trimethylamine into ammonium nitrate particles. *J. Phys. Chem. A* **2009**, *113*, 4840−4843.
(37) Bzdek, B. R.; Ridge, D. P.; Johnston, M. V. Amine exchange into ammonium bisulfate and ammonium nitrate nuclei. *Atmos. Chem. Phys.* **2010**, *10*, 3495−3503.
(38) Yu, H.; McGraw, R.; Lee, S.-H. Effects of amines on formation of sub-3nm particles and their subsequent growth. *Geophys. Res. Lett.* **2012**, *39*, L02807.
(39) Almeida, J.; Schobesberger, S.; Kürten, A.; Ortega, I. K.; Kupiainen-Määttä, O.; Prapian, A. P.; Adamov, A.; Amorim, A.; Bianchi, F.; Breitenlechner, M.; et al. Molecular understanding of sulphuric acid−amine particle nucleation in the atmosphere. *Nature* **2013**, DOI: 10.1038/nature12663.
(40) McGrath, M. J.; Olenius, T.; Ortega, I. K.; Loukonen, V.; Paasonen, P.; Kürten, T.; Kulmala, M.; Vehkamaki, H. Atmospheric cluster dynamics code: a flexible method for solution of the birth-death equations. *Atmos. Chem. Phys.* **2012**, *12*, 2345−2355.
(41) Ortega, I. K.; Kupiainen, O.; Kürten, T.; Olenius, T.; Wilkman, O.; McGrath, M. J.; Loukonen, V.; Vehkamaki, H. From quantum chemical formation free energies to evaporation rates. *Atmos. Chem. Phys.* **2012**, *12*, 225−235.
(42) Diamant, R. M. E. *The Chemistry of Building Materials*; Business Books Limited: London, 1970.
(43) Hodge, E. M.; Diamond, M. L.; McCarry, B. E.; Stern, G. A.; Harper, P. A. Sticky windows: chemical and biological characteristics of the organic film derived from particulate and gas-phase air contaminants found on an urban impervious surface. *Arch. Environ. Contam. Toxicol.* **2003**, *44*, 421−429.
(44) Lam, B.; Diamond, M. L.; Simpson, A. J.; Makar, P. A.; Truong, J.; Hernandez-Martinez, N. A. Chemical composition of surface films on glass windows and implications for atmospheric chemistry. *Atmos. Environ.* **2005**, *39*, 6578−6586.
(45) Vogt, R.; Finlayson-Pitts, B. J. A diffuse-reflectance infrared Fourier-transform spectroscopic (DRIFTS) study of the surface-reaction of NaCl with gaseous NO_2 and HNO_3. *J. Phys. Chem. A* **1994**, *98*, 3747−3755.
(46) Karagulian, F.; Lea, A. S.; Dilbeck, C. W.; Finlayson-Pitts, B. J. A new mechanism for ozonolysis of unsaturated organics on solids: phosphocholines on NaCl as a model for sea salt particles. *Phys. Chem. Chem. Phys.* **2008**, *10*, 528−541.
(47) Dawson, M. L.; Perraud, V.; Ezell, M. J.; Finlayson-Pitts, B. J. A simple method for measurement of gas-phase ammonia and amines in air. In preparation.
(48) Perman, E. P. Vapour pressure of aqueous ammonia solution Part II. *J. Chem. Soc.* **1903**, *83*, 1168−1184.
(49) Gruvin, B. E.; Johansson, T.; Hatcher, M. E. Low-temperature oxidation of silicon powders. *Mater. Sci. Eng.* **1985**, *71*, 363−367.
(50) Tichapondwa, S. M.; Focke, W. W.; Del Fabbro, O.; Muller, E. Suppressing hydrogen evolution by aqueous silicon powder dispersions by controlled silicon surface oxidation. *Propellants Explos., Pyrotech.* **2013**, *38*, 48−55.

(51) Mihalopoulos, N.; Barnes, I.; Becker, K. H. Infrared-absorption spectra and integrated band intensities for gaseous methanesulfonic-acid (MSA). *Atmos. Environ. Part A* **1992**, *26*, 807−812.
(52) Givan, A.; Loewenschuss, A.; Nielsen, C. J. Infrared spectrum and ab initio calculations of matrix isolated methanesulfonic acid species and its 1:1 water complex. *J. Mol. Struct.* **2005**, *748*, 77−90.
(53) Maiorov, V. D.; Voloshenko, G. I.; Librovich, N. B. Ion-molecular interactions in solutions of methanesulfonic acid in diethylamine according to IR spectroscopy data. *Russ. J. Phys. Chem. B* **2011**, *5*, 271−277.
(54) Davydov, V. Y.; Kiselev, A. V.; Zhuravle, L. T. Study of surface and bulk hydroxyl groups of silica by infra-red spectra and D_2O-exchange. *Trans. Far. Soc.* **1964**, *60*, 2254−2264.
(55) Kiselev, A. V. *Infrared spectra of surface compounds*; John Wiley & Sons: New York, 1975.
(56) Hoffmann, P.; Knozinger, E. Novel aspects of mid and far IR Fourier spectroscopy applied to surface and adsorption studies on SiO_2. *Surf. Sci.* **1987**, *188*, 181−198.
(57) Tolbert, M. A.; Middlebrook, A. M. Fourier-transform infrared studies of model polar stratospheric cloud surfaces—growth and evaporation of ice and nitric-acid ice. *J. Geophys. Res.* **1990**, *95*, 22423−22431.
(58) Ritzhaupt, G.; Devlin, J. P. Infrared-spectra of nitric and hydrochloric-acid hydrate thin-films. *J. Phys. Chem.* **1991**, *95*, 90−95.
(59) Smith, R. H.; Leu, M. T.; Keyser, L. F. Infrared-spectra of solid films formed from vapors containing water and nitric-acid. *J. Phys. Chem.* **1991**, *95*, 5924−5930.
(60) Ramazan, K. A.; Wingen, L. M.; Miller, Y.; Chaban, G. M.; Gerber, R. B.; Xantheas, S. S.; Finlayson-Pitts, B. J. New experimental and theoretical approach to the heterogeneous hydrolysis of NO_2: Key role of molecular nitric acid and its complexes. *J. Phys. Chem. A* **2006**, *110*, 6886−6897.
(61) Lucovsky, G. Chemical effects on the frequencies of Si−H vibrations in amorphous solids. *Solid State Commun.* **1979**, *29*, 571−576.
(62) Shanks, H.; Fang, C. J.; Ley, L.; Cardona, M.; Demond, F. J.; Kalbitzer, S. Infrared-spectrum and structure of hydrogenated amorphous-silicon. *Phys. Status Solidi B* **1980**, *100*, 43−56.
(63) Tsu, D. V.; Lucovsky, G.; Davidson, B. N. Effects of the nearest neighbors and the alloy matrix on SiH stretching vibrations in the amorphous SiO_r:H ($0 < r < 2$) alloy system. *Phys. Rev. B* **1989**, *40*, 1795−1805.
(64) Murphy, W. F.; Zerbetto, F.; Duncan, J. L.; McKean, D. C. Vibrational-spectrum and harmonic force-field of trimethylamine. *J. Phys. Chem.* **1993**, *97*, 581−595.
(65) Nersasian, A.; Johnson, P. R. Infrared spectra of alkanesulfonic acids, chlorosulfonated polyethylene and their derivatives. *J. Appl. Polym. Sci.* **1965**, *9*, 1653−1668.
(66) Tuttolomondo, M. E.; Navarro, A.; Pena, T.; Varetti, E. L.; Parker, S. F.; Ben Altabef, A. Conformational and vibrational analysis of methyl methanesulfonate, $CH_3SO_2OCH_3$. *J. Phys. Chem. A* **2009**, *113*, 8401−8408.
(67) Socrates, G. *Infrared and Raman characteristic group frequencies*; John Wiley & Sons Ltd: New York, 2001.
(68) Finlayson-Pitts, B. J.; Wingen, L. M.; Sumner, A. L.; Syomin, D.; Ramazan, K. A. The heterogeneous hydrolysis of NO_2 in laboratory systems and in outdoor and indoor atmospheres: An integrated mechanism. *Phys. Chem. Chem. Phys.* **2003**, *5*, 223−242.
(69) Qiu, C.; Wang, L.; Lal, V.; Khalizov, A. F.; Zhang, R. Y. Heterogeneous reactions of alkylamines with ammonium sulfate and ammonium bisulfate. *Environ. Sci. Technol.* **2011**, *45*, 4748−4755.
(70) Theoret, A.; Sandorfy, C. Infrared spectra + crystalline phase transitions of ammonium nitrate. *Can. J. Chem.* **1964**, *42*, 57−62.
(71) Fernandes, J. R.; Ganguly, S.; Rao, C. N. R. Infrared spectroscopic study of the phase-transitions in $CSNO_3$, $RBNO_3$, and NH_4NO_3. *Spectrochim. Acta Part A* **1979**, *35*, 1013−1020.
(72) Davis, K. M.; Tomozawa, M. An infrared spectroscopic study of water-related species in silica glasses. *J. Non-Cryst. Solids* **1996**, *201*, 177−198.
(73) Moussa, S. G.; McIntire, T. M.; Szori, M.; Roeselova, M.; Tobias, D. J.; Grimm, R. L.; Hemminger, J. C.; Finlayson-Pitts, B. J. Experimental and theoretical characterization of adsorbed water on self-assembled monolayers: Understanding the interaction of water with atmospherically relevant surfaces. *J. Phys. Chem. A* **2009**, *113*, 2060−2069.
(74) Sumner, A. L.; Menke, E. J.; Dubowski, Y.; Newberg, J. T.; Penner, R. M.; Hemminger, J. C.; Wingen, L. M.; Brauers, T.; Finlayson-Pitts, B. J. The nature of water on surfaces of laboratory systems and implications for heterogeneous chemistry in the troposphere. *Phys. Chem. Chem. Phys.* **2004**, *6*, 604−613.
(75) Wang, L.; Lal, V.; Khalizov, A. F.; Zhang, R. Heterogeneous chemistry of alkylamines with sulfuric acid: Implications for atmospheric formation of alkylaminium sulfates. *Environ. Sci. Technol.* **2010**, *44*, 2461−2465.
(76) Sellegri, K.; Umann, B.; Hanke, M.; Arnold, F. Deployment of a ground-based CIMS apparatus for the detection of organic gases in the boreal forest during the QUEST campaign. *Atmos. Chem. Phys.* **2005**, *5*, 357−372.
(77) Akyuz, M. Simultaneous determination of aliphatic and aromatic amines in ambient air and airborne particulate matters by gas chromatography-mass spectrometry. *Atmos. Environ.* **2008**, *42*, 3809−3819.
(78) Yu, H.; Lee, S.-H. Chemical ionisation mass spectrometry for the measurement of atmospheric amines. *Environ. Chem.* **2012**, *9*, 190−201.
(79) Huang, G.; Hou, J.; Zhou, X. A measurement method for atmospheric ammonia and primary amines based on aqueous sampling, OPA derivatization and HPLC analysis. *Environ. Sci. Technol.* **2009**, *43*, 5851−5856.
(80) Hanson, D. R.; McMurry, P. H.; Jiang, J.; Tanner, D.; Huey, L. G. Ambient pressure proton transfer mass spectrometry: Detection of amines and ammonia. *Environ. Sci. Technol.* **2011**, *45*, 8881−8888.
(81) Lawler, M. J.; Sander, R.; Carpenter, L. J.; Lee, J. D.; von Glasow, R.; Sommariva, R.; Saltzman, E. S. HOCl and Cl_2 observations in marine air. *Atmos. Chem. Phys.* **2011**, *11*, 7617−7628.
(82) Knipping, E. M.; Dabdub, D. Impact of chlorine emissions from sea-salt aerosol on coastal urban ozone. *Environ. Sci. Technol.* **2003**, *37*, 275−284.
(83) Vutukuru, S.; Dabdub, D. Modeling the effects of ship emissions on coastal air quality: A case study of southern California. *Atmos. Environ.* **2008**, *42*, 3751−3764.
(84) Atkinson, R.; Perry, R. A.; Pitts, J. N., Jr. Rate constants for the reactions of the OH radical with $(CH_3)_2NH$, $(CH_3)_3N$, and $C_2H_5NH_2$ over the temperature range 298−426 K. *J. Chem. Phys.* **1978**, *68*, 1850−1853.
(85) Tuazon, E. C.; Atkinson, R.; Aschmann, S. M.; Arey, J. Kinetics and products of the gas-phase reactions of O_3 with amines and related compounds. *Res. Chem. Intermed.* **1994**, *20*, 303−320.